ELSEVIER

Inorganica Chimica Acta 229 (1995) 143–151

Inorganica Chimica Acta

Metal–metal interaction in ligand-bridged dimolybdenum(0,0) and -(I,0) complexes with very small frontier orbital gaps: electrochemistry and spectroscopic properties of three neighboring oxidation states ☆

Wolfgang Kaim [a,*], Wolfgang Bruns [a], Stephan Kohlmann [a], Michael Krejčik [b]

[a] *Institut für Anorganische Chemie der Universität, Pfaffenwaldring 55, D-70550 Stuttgart, Germany*

[b] *Heyrovsky Institute of Physical Chemistry, Academy of Sciences of the Czech Republic, Dolejškova 3, CZ-18223 Prague, Czech Republic*

Received 26 May 1994; revised 26 July 1994

Abstract

Complexes ($(\mu\text{-L})[Mo(CO)_2(P^nBu_3)_2]_2$) with *cis*-carbonyl ligands and symmetrically bridging bis(α-diimine) chelate ligands L = 2,2′-bipyrimidine (bpym) and 2,5-bis(2-pyridyl)pyrazine (2,5-bppz) were synthesized and studied in different oxidation states by cyclic voltammetry, ^{1}H NMR, EPR, IR and UV–Vis–NIR absorption spectroscopy. The combination of two very electron rich d^6 metal centers with one π accepting bridging ligand results in rather small HOMO–LUMO energy gaps, as evident from differences of about 1 V between the potentials for reversible oxidation and reduction and from intense charge transfer absorptions at about 1 eV, i.e. in the near-infrared (NIR) region. Whereas the shifts of the carbonyl vibrational bands are about equal for the reduction (low-energy shift) and the oxidation (high-energy shift) of the more stable bpym complex, the EPR results reveal occupation of the α-diimine π^* orbitals in the anionic forms and an Mo(I)/Mo(0) mixed-valent state with a comproportionation constant K_c greater than 10^8 for the cation $\{(bpym)[Mo(CO)_2(P^nBu_3)_2]_2\}^+$. Electronic transitions observed by UV–Vis–IR spectroelectrochemistry confirm these assignments of the redox orbitals; the maximum of the weak metal-to-metal charge transfer band of the mixed-valent complex $\{(bpym)[Mo(CO)_2(P^nBu_3)_2]_2\}^+$ was found at 3700 nm (2700 cm^{-1}).

Keywords: Electrochemistry; Molybdenum complexes; Bridging ligand complexes; Dinuclear complexes; Spectroelectrochemistry

1. Introduction

Compounds with efficient narrow-band absorption of near-infrared (NIR) radiation are of interest as dyes for diode lasers and corresponding applications in information technology [1–3]. One possible way to construct such species is to use metal complexes with intense charge transfer transitions [1,3]. In particular, metal-to-ligand charge transfer (MLCT) excited states are attractive for photophysical applications because they are known to be relatively inert with respect to dissociation [4]. Long-wavelength MLCT bands require

(i) one or more very electron rich metal center(s),

(ii) an acceptor ligand with rather low-lying unoccupied orbitals, and

(iii) a kind of interaction (e.g. via π orbital overlap) between metal and ligand which is strong enough to allow intense NIR absorption without causing a too large energy splitting of metal and ligand π orbitals. Polynuclear complexes with bridging acceptor ligands can display two additional effects for narrowing the HOMO–LUMO gap [3b], viz.,

(iv) the metal–metal interaction can split the donor levels, thereby destabilizing the HOMO [5], and

(v) multiple metal coordination can further stabilize the π^* orbitals, in particular the LUMO of the acceptor ligands [6].

In the following we describe two dinuclear Mo(0) complexes, **1** and **2**, which meet all requirements (i)–(v). *cis*-Dicarbonylbis(trialkylphosphine)molybdenum(0) is known to be an electron rich metal complex fragment which can bind to aromatic and non-aromatic α-diimines [7–9] and related unsaturated chelate ligands such as

---

☆ This paper is dedicated to Professor F.A. Cotton on the occasion of his 65th birthday.

* Corresponding author.

SSDI 0020-1693(94)04239-R

tetraaza-1,3-dienes [10]. On the ligand side, 2,2′-bipyrimidine (bpym) and 2,5-bis(2-pyridyl)pyrazine(2,5-bppz) are compounds which have rather low lying π^* orbitals and which can form symmetrically dinuclear complexes with modest ligand-mediated metal–metal interaction [11–15]. The relatively small π^* molecular orbital coefficients at the coordinating nitrogen centers of bpym and 2,5-bppz [11] ensure that requirement (iii) is fulfilled; accordingly, the previously reported mononuclear complex (bpym)Mo(CO)$_2$(PR$_3$)$_2$, R = n-butyl, already showed a bathochromically shifted MLCT absorption with respect to other related compounds [8]. In contrast, ligands L with large π^* MO coefficients such as 2,2′-bipyrazine [8], 3,3′-bipyridazine [8], 1,4-diazadienes [7,9] or tetraazadienes [10] have yielded complexes (L)Mo(CO)$_2$(PR$_3$)$_2$ with relatively high energy charge transfer transitions.

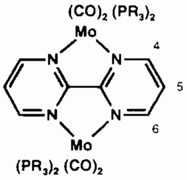

1

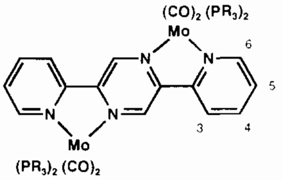

2

R = n - C_4H_9

In addition to the optical absorption data of complexes **1** and **2** and, in the case of the more stable system **1**, of its neighboring oxidation states, we report their electrochemistry, ^{1}H NMR and IR spectroscopy and the EPR of paramagnetic forms in order to confirm the MLCT character of the long-wavelength transitions. In particular, the singly oxidized species $\{(\text{bpym})[\text{Mo(CO)}_2(\text{PR}_3)_2]_2\}^+$ ($\mathbf{1}^+$) is an Mo(I)/Mo(0) (d^5/d^6) mixed-valent complex; there are few examples for this particular oxidation state combination [16–18] and for mixed-valent dimolybdenum species in general [17,19,20] while the related Ru(III)/Ru(II) systems are very well established [5,12,21–24].

2. Results

Complexes **1** and **2** were obtained as fairly labile but isolable species by the stepwise reaction of two equivalents of Mo(CO)$_2$(CH$_3$CN)(PBu$_3$)$_3$ with the free bis(α-diimine) ligands in hexane. The ^{1}H NMR spectra recorded in non-coordinating C$_6$D$_6$ confirm the symmetrically dinuclear arrangement (Fig. 1, Table 1); well separated doublets in the carbonyl vibrational spectra (Fig. 2,, Table 2) further indicate the presence of symmetrical species with *cis*-carbonyl configuration [7–10].

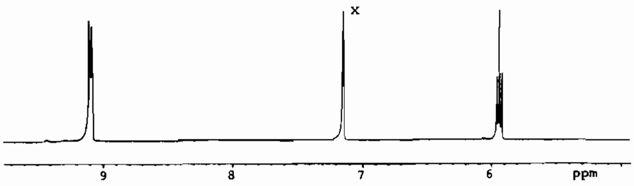

Fig. 1. ^{1}H NMR spectrum of complex **1** in C$_6$D$_6$ (×: solvent signal).

Table 1
^{1}H NMR data of ligands and complexes

Compound	δ (ppm)		J (Hz)
	α-diimine	P(n-Bu$_3$) [b]	
bpym [a]	8.32 (H4,6; d) 6.21 (H5; t)		4.8
1 [a]	9.10 (H4,6; d) 5.94 (H5; t)	1.37 (PCH$_2$) 1.25 (CH$_3$) 0.89 (CH$_3$)	5.3
2,5-bppz [c]	8.45 (H3; d) 7.86 (H4; dd) 7.37 (H5; dd) 8.74 (H6; d) 9.66 (H$_{pz}$; s)		8.3 (H3/H4) 7.2 (H4/H5) 5.5 (H5/H6)
2 [a]	7.95 (H3; d) 6.85 (H4; dd) 6.43 (H5; dd) 9.50 (H6; d) 9.99 (H$_{pz}$; s)	1.47 (PCH$_2$) 1.33 (CH$_2$) 0.80 (CH$_3$)	8.3 (H3/H4) 7.5 (H4/H5) 5.6 (H5/H6)

[a] From measurements in C$_6$D$_6$.
[b] Multiplet signals.
[c] In CDCl$_3$.

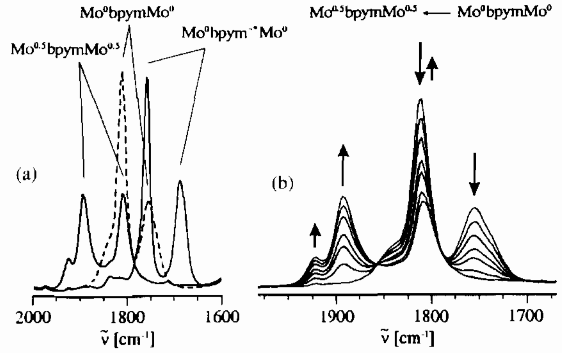

Fig. 2. (a) IR spectra in the CO stretching region for the redox system $\mathbf{1}^{-/0/+}$ as obtained by FTIR spectroelectrochemistry in CH$_2$Cl$_2$/0.1 M Bu$_4$NPF$_6$. (b) Spectral changes during the conversion $\mathbf{1}^0 \rightarrow \mathbf{1}^+$.

Table 2
Carbonyl vibrational data from IR spectra

Complex	$\tilde{\nu}$(CO) (cm^{-1})		Medium
	b_{1u}	b_{2u}	
1	1840	1785	hexane
1	1811 [a]	1754	CH$_2$Cl$_2$/0.1 M Bu$_4$NPF$_6$
$\mathbf{1}^+$	1891 [b]	1808	CH$_2$Cl$_2$/0.1 M Bu$_4$NPF$_6$
$\mathbf{1}^-$	1757	1684	CH$_2$Cl$_2$/0.1 M Bu$_4$NPF$_6$
2	1815	1770	hexane

[a] Shoulder at 1840 cm^{-1}.
[b] Reduced intensity, additional small band at 1921 cm^{-1}.

Although rather labile, complexes **1** and **2** show quite reversible waves of equal intensity for the first oxidation and reduction steps in their cyclovoltammograms (Fig. 3, Table 3). Processes beyond the first oxidation and reduction are irreversible; in particular, there is a large, essentially irreversible oxidation wave at about +0.27 V versus SCE (Fig. 3).

The monoanionic and monocationic paramagnetic states could be generated electrochemically or chemically, e.g. via reduction with K, in order to be studied by EPR spectroscopy (Fig. 4, Table 4). The anions $\mathbf{1}^{\bullet -}$ and $\mathbf{2}^{\bullet -}$ gave extensively hyperfine-structured EPR spectra which are typical for anion radical complexes [25] and which can be simulated (Fig. 4) using established (bpym$^{\bullet -}$, [26]) or calculated hyperfine parameters. For the anion radical of the 2,5-bppz ligand with at least seven different coupling nuclei we carried out a Hückel MO/McLachlan [27] perturbation calculation of the π spin populations (Fig. 5), the variation of the Coulomb integral parameter h_N reflecting the effect of double chelate coordination by electrophilic metal centers [25,26]. According to these results we made the tentative assignments of coupling constants for $\{(2,5\text{-bppz})[\mathrm{Mo(CO_4]_2}\}^{\bullet -}$ as listed in Table 4; the spectrum of $\mathbf{2}^{\bullet -}$ with additional ^{31}P coupling and a total of 30 375 theoretical lines (!) could not be fully analyzed.

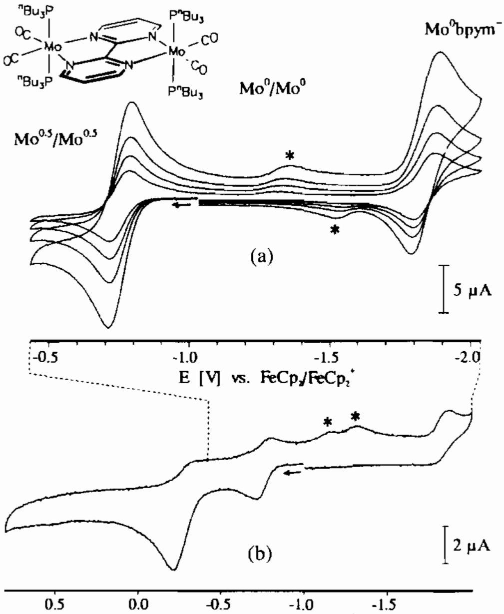

Fig. 3. (a) Cyclic voltammograms of complex **1** in CH_2Cl_2/0.1 M Bu_4NClO_4 at 50, 100, 200 and 500 mV s^{-1} scan rate. (b) Extended potential scale, showing the irreversible second oxidation at 100 mV s^{-1}. (*: signals due to decomposition products).

Table 3
Electrochemical data [a] of ligands and complexes

Compound	E_{red} (1e)	E_{ox1} (1e)	E_{ox2}	Solvent [b]
bpym	−1.73 (80)			DMF
1	−1.37 (80)	−0.28 (60)	+0.27 [c]	CH_2Cl_2 or DCE
2,5-bppz	−1.49 (80)			DMF
2	−1.46 (100)	−0.40 (170)	+0.27 [c]	DCE

[a] Potentials in V vs. SCE from cyclic voltammetry at 100 mV s^{-1} scan rate. Peak potential differences (in mV) in parentheses.

[b] 0.1 M Bu_4NClO_4 as electrolyte; DCE = 1,2-dichloroethane.

[c] Peak potential for irreversible process with high anodic current (see Fig. 3).

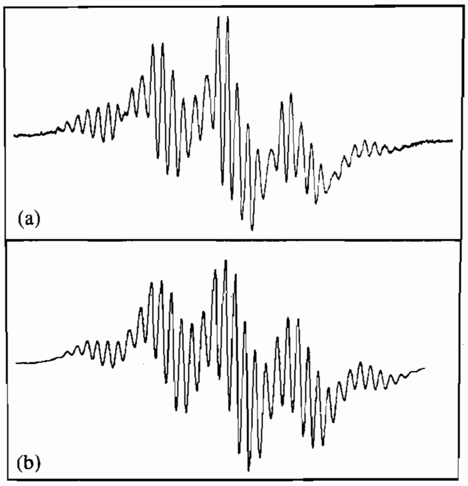

Fig. 4. (a) EPR spectrum of $\mathbf{1}^{\bullet -}$ at 295 K in THF solution. (b) Computer-simulated spectrum with the data from Table 4 and 0.06 mT linewidth.

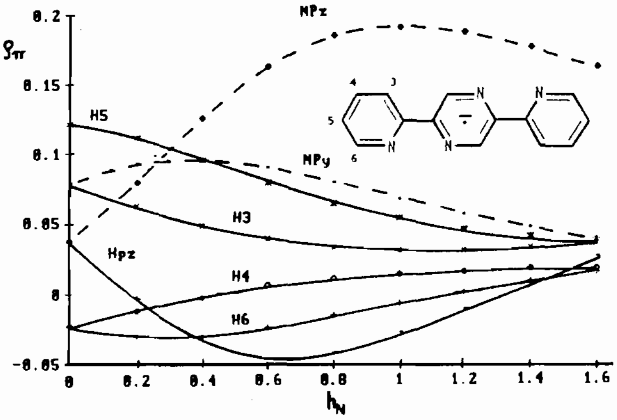

Fig. 5. π spin populations ρ_π for 2,5-bppz radical anion from HMO/McLachlan calculations, using the Coulomb integral value h_N of the four nitrogen centers as perturbation parameter.

In contrast to the monoanionic species, the cation $\mathbf{1}^{\bullet +}$ displayed an intense EPR signal only in the frozen state; this and the almost axial g anisotropy at low temperatures with $g_{1,2} > 2$ and $g_3 < 2$ are characteristic features of mixed-valent d^5/d^6 species [18,23,28].

Use of a spectroelectrochemical cell [29] allowed us to study the carbonyl vibrational and UV–Vis–NIR absorption spectra of the more stable two-step reversible redox system $\mathbf{1}^{-/0/+}$. The carbonyl stretching bands are shifted by almost equal amounts to lower (anion) or higher (cation) energies (Fig. 2, Table 2); re-generation of **1** and the presence of isosbestic points confirm the

Table 4
EPR data of paramagnetic species [a]

Complex	g	a (mT)		
		^{31}P	^{14}N	^{1}H
$\mathrm{bpym^{\bullet -}}$ [b]	2.0030		0.143	0.492 (H5) 0.015 (H4,6)
$\mathrm{(bpym^{\bullet -})[Mo(CO)_4]_2}$ [b,c]	2.0023		0.228	0.495 (H5) 0.053 (H4,6)
1$^-$	2.0011 [d]	1.440	0.225	0.450 (H5) [f] (H4,6)
$\mathrm{(2,5\text{-}bppz^{\bullet -})[Mo(CO)_4]_2}$ [e]	2.0028		0.374 (pz) 0.163 (py)	0.163 (H5) 0.108 (H3, $\mathrm{H_{pz}}$) 0.052 (H6)
2$^-$	2.0020	1.650	[f]	[f]
1$^+$	2.117 [g]	[f]	[f]	[f]

[a] Measurements for anion radicals at room temperature in THF solution.
[b] From Ref. [26].
[c] $a(^{95,97}\mathrm{Mo}) = 0.105$ mT.
[d] No g anisotropy observed at 110 K.
[e] Tentative assignments based on MO calculated π spin populations (Fig. 5).
[f] Not sufficiently resolved.
[g] From electrochemical oxidation in $\mathrm{CH_2Cl_2/0.1\ M\ Bu_4NPF_6}$: $g_1 = 2.216$, $g_2 = 2.16$, $g_3 = 1.97$ at 110 K.

reversible nature of the electron transfer equilibria. In the electron absorption spectra, both neutral complexes exhibit intense charge transfer bands at very low energies in the NIR region (Fig. 6, Table 5); one-electron reduction and oxidation of **1** caused these features to disappear. While reduction produces bands typical for $\mathrm{bpym^{\bullet -}}$ and its complexes [30], the one-electron oxidation of **1** results in the formation of new bands at 800 and 543 nm; the expected [18,21–23,31] intervalence or metal-to-metal charge transfer (MMCT) band could not be observed in the region between 800 and 2500 nm. However, a careful inspection of the FTIR spectra (Fig. 7) from spectroelectrochemistry in the mid-infrared (MIR) region [32] revealed the reversible appearance of a broad hump on oxidation (Table 5).

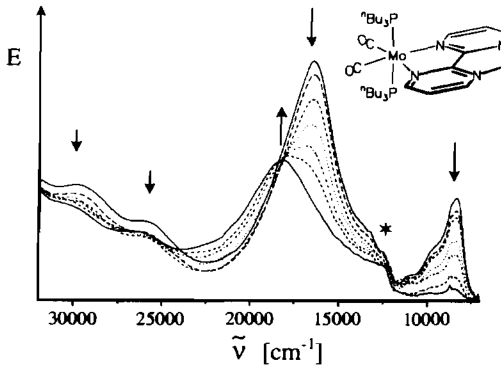

Fig. 6. UV–Vis–NIR spectra from spectroelectrochemistry of $\mathbf{1}^0 \rightarrow \mathbf{1}^+$ in $\mathrm{CH_2Cl_2/0.1\ M\ Bu_4NPF_6}$. (*: detector switching).

3. Discussion

3.1. Spectroscopy of neutral complexes

Complexes **1** and **2** were synthesized via a standard procedure as well soluble but rather labile and air-sensitive materials. The $\mathrm{P^nBu_3}$ ligands which were used in order to avoid the common problem of poor solubility of dinuclear complexes [18c] created difficulties in the crystallization of compound **2**; this complex also showed very high dissociative lability, presumably due to the non-equivalent coordination of individual molybdenum centers by the pyridine and pyrazine nitrogen atoms.

^{1}H NMR and carbonyl vibrational spectra confirm the typical [7–10] *cis*-carbonyl/*trans*-phosphine arrangement in symmetrically dinuclear complexes (cf. Fig. 3). The comparatively [7–10] low values of $\tilde{\nu}(\mathrm{CO}) < 1850$ cm^{-1} for the neutral complexes illustrate the moderate [11] π acceptor capability of the bpym and 2,5-bppz ligands, rendering the Mo(0) centers still fairly electron-rich. A comparison of the solvent-dependent values of the neutral complexes confirms that the 2,5-bppz ligand is a slightly poorer π acceptor ligand in that situation than bpym. On the other hand, the spread-out chemical shifts for the 'aromatic' protons already suggest that there are close-lying (metal-to-ligand) charge transfer excited states present. In particular, the two kinds of protons of the dinucleating bpym ligand in **1** are quite separate from each other in the ^{1}H NMR spectrum (Fig. 1). The protons H(4,4′,6,6′) at carbon π centers with a very small negative spin density in the reduced state ($\pi_1^* = \mathrm{b_{2u}}$ singly occupied [26]) are shifted downfield to $\delta > 9$ ppm whereas the nuclei H(5,5′) are shifted

Table 5
Electronic absorption data for dimolybdenum complexes

Complex	λ_{max} (nm)			Solvent
	MLCT1	MLCT2	'LF' [a]	
(bpym)[Mo(CO)$_4$]$_2$	670	452	392	toluene
1	1212, 1030sh	611	390	toluene
1	1195, 1025sh	604	388	CH$_2$Cl$_2$/0.1 M Bu$_4$NPF$_6$
1^{+} [b]	800sh	543	375	CH$_2$Cl$_2$/0.1 M Bu$_4$NPF$_6$
(2,5-bppz)[Mo(CO)$_4$]$_2$ [c]	695	490		toluene
2	1350, 1140sh	795	530	toluene
	$\pi(7) \rightarrow \pi(9)$ [d]	$\pi(7) \rightarrow \pi(10)$	$\pi(6) \rightarrow \pi(7)$	
(bpym$^{\bullet -}$)[Mo(CO)$_4$]$_2$ [d]	819	480	356	DMF/0.1 M Bu$_4$NBF$_6$
1^{-}	820	495	350	CH$_2$Cl$_2$/0.1 M Bu$_4$NPF$_6$

[a] Solvent-independent 'ligand-field' transition (tentative assignment, see Refs. [34,35]).

[b] Additional band (MMCT) at 3700 nm ($\Delta\nu_{1/2}$ 1300 cm^{-1}).

[c] From Ref. [11].

[d] Values and assignments as intra-ligand (IL) transitions from Ref. [30].

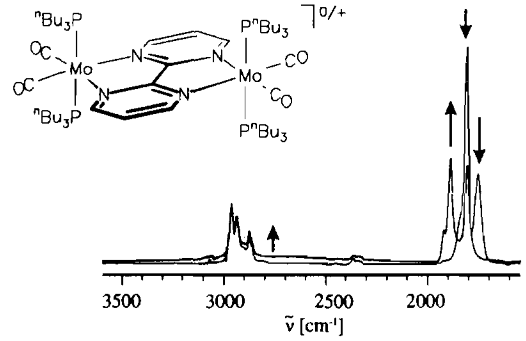

Fig. 7. NIR–MIR spectra from FTIR spectroelectrochemistry of $\mathbf{1}^0 \rightarrow \mathbf{1}^+$ in CH$_2$Cl$_2$/0.1 M Bu$_4$NPF$_6$.

upfield to $\delta < 6$ ppm. The carbon π centers in 5,5′ (*para*) position are known to exhibit a rather large spin density in the anion radical state as evident from EPR spectroscopy [26]; the contributions from close-lying paramagnetic excited states [33] are therefore believed to be quite strong for these compounds.

As expected [3b,7–9] for systems with long-wavelength MLCT transitions, the replacement of Mo(CO)$_4$ by the more electron rich Mo(CO)$_2$(P^{n}Bu$_3$)$_2$ fragment drastically lowers the energy of those transitions. The MLCT1 bands now lie in the NIR region, shifted by 7000 cm^{-1} and thus reduced to about one half in energy at the absorption maximum; these bands are resolved into a main absorption feature ($d \rightarrow \pi^*$ [13,34]) and a clearly visible high-energy shoulder. This shoulder can be assigned either to an overlap-disfavored transition from a different d orbital [9] or to the transition from a different combination of d orbitals [13], considering the possibility of metal–metal (d–d) interaction across the bpym ligand (see below).

The second, more intense MLCT2 bands are also bathochromically shifted in the dicarbonyl complexes relative to the tetracarbonyl analogues albeit to different extents, viz., by about 5750 cm^{-1} for the bpym system and by almost 8000 cm^{-1} for the complexes of 2,5-bppz. This result and the fact that the solvent insensitive band ('ligand field (LF) transition' [35]) of bpym complexes at about 390 nm remains unchanged lead to a clear separation of the major absorption bands which are considerably overlapping in the tetracarbonylmetal analogues [13,34,35]. In view of the certainly diminished ligand field splitting of the dicarbonyl relative to the tetracarbonyl complexes the assignment of the rather intense 390 nm feature to an LF transition [35] seems quite unlikely. Further arguments for assignments in the particularly intricate bpym system [13,34] are based on spectroelectrochemical results which will be discussed below.

3.2. Electrochemistry

The dinuclear complexes **1** and **2** exist only in a remarkably narrow electrochemical potential range of less than 1.1 V; they are reduced and especially oxidized at easily accessible potentials. The reductions are typical one-electron processes of coordinated heterocyclic ligands [11] as confirmed by EPR spectra of the resulting anions (see Fig. 4); the potentials are slightly more positive than those of the corresponding free ligands but distinctly more negative than the values of dinuclear bpym and 2,5-bppz complexes with the less electron-rich tetracarbonylmolybdenum fragment [11]. This result indicates that the π backdonation from Mo(CO)$_2$(P^{n}Bu$_3$)$_2$ almost compensates [18a] for the polarizing σ acceptor effect of the electrophilic metal centers.

The first oxidation waves with the same current intensity as the ligand-centered one-electron reduction signals have to be interpreted as a conversion to mixed-valent, i.e. Mo(I)/Mo(0) cations. While d^5/d^6 mixed-valent dimers are well established for the elements of Group 8, the number of Mo(I)/Mo(0) species is quite limited [16–18]. The expected second oxidation wave to the Mo(I)/Mo(I) state is assumed to lie within the intense, largely irreversible wave at about +0.27 V versus SCE (Fig. 3).

According to Eq. (1), the difference between the anodic peak potentials for first and second oxidation of **1** yields an estimate for the comproportionation constant K_c of 6×10^8. This value is much larger than the $K_c=5\times10^2$ determined for the related bpym-bridged $4d^5/4d^6$ dimer $\{(\mathrm{bpym})[\mathrm{Ru(bpy)_2}]_2\}^{5+}$ [12,36], a result which suggests considerably stronger metal/bpym/metal (d/π*/d) orbital interaction [5] in the case of the low-valent molybdenum fragments with their very much destabilized 4d orbitals.

$$K_c=[\mathrm{M}^+]^2/[\mathrm{M}][\mathrm{M}^{2+}]$$

$$\log K_c=\Delta E/0.059\ \mathrm{V} \qquad (1)$$

The slightly less negative value of the oxidation potential for **1** relative to **2** reflects the stronger donor ligand bpym [6,11] with its symmetrical chelate coordination; asymmetrical coordination of the individual metal centers by the 2,5-bppz ligand may weaken the metal–ligand bonds in **2**.

In agreement with previous practice [6,11,18c,37], the energies E_{op} of the long-wavelength absorption bands (MLCT1) can be correlated with the separations $E_{\mathrm{ox1}}-E_{\mathrm{red}}=\Delta E_{\mathrm{red/ox}}$, the remaining difference χ in approximation (2) being ascribed to contributions from intra- and intermolecular reorganization after 'vertical' optical excitation.

$$E_{\mathrm{op}}\ (\text{in eV})=\Delta E_{\mathrm{red/ox}}\ (\text{in V})+\chi \qquad (2)$$

When comparing electrochemical and spectroscopic data (Tables 3 and 5) for complexes **1** and **2**, the χ values come out unexpectedly as small *negative* numbers (−0.05 and −0.14 (e)V, respectively), indicating the approximative nature of relation (2); an alternative explanation based on two *different* π* orbitals involved [34] is given further below. In any case, the correlations of optical and electrochemical data suggest a small reorganization energy which is not unexpected in view of similar observations for the related complexes $(\mu\text{-L})[\mathrm{M(CO)_3(P^iPr_3)_2}]_2$, L = pyrazine or 4,4′-bipyridine; M = Mo, W [18c].

3.3. EPR and UV–Vis–IR spectroelectrochemistry

Unambiguous information about the oxidation state distribution in paramagnetic species, including radical ion complexes [25,38] and mixed-valent systems [39], can be obtained from EPR spectroscopy. In fact, complex **1** is one of the few well-documented examples in metal carbonyl chemistry where reversible one-electron reduction and oxidation allow the exact determination of the kind of frontier or 'redox' orbitals and thus, in the one-electron approximation, the MLCT nature of the lowest lying excited state.

The anion radical complex $\mathbf{1}^{\bullet-}=(\mathrm{bpym}^{\bullet-})$-$[\mathrm{Mo^0(CO)_2(P^nBu_3)_2}]_2$ has EPR characteristics similar to those of the bis(tetracarbonylmolybdenum) analogue [26], with the addition of a quintet hyperfine splitting from four equivalent ^{31}P nuclei (Fig. 4, Table 4). The magnitude of that splitting in $\mathbf{1}^{\bullet-}$ and $\mathbf{2}^{\bullet-}$ is in the expected range for systems with $\mathrm{M{-}PR_3}$ bonds parallel to the π system representing the singly occupied molecular orbital (SOMO) [7,8,18c]; the $a(^{31}\mathrm{P})$ splitting for $\mathbf{1}^{\bullet-}$ is only slightly smaller than the value of 1.593 mT [8] for the corresponding mononuclear radical complex. Both anion radical complexes show the expected [25] decrease of the *g* factor due to the presence of triorganophosphine ligands with their low-lying unoccupied orbitals [8,40].

While the anionic complexes did not exhibit a detectable *g* anisotropy in frozen solution, the low-temperature spectrum of the cationic species $\mathbf{1}^+$ shows an essentially axial signal without ligand hyperfine splitting. The perpendicular features of the *g* tensor components (g_1 and g_2 in Table 4) are distinctly higher than those ($g_\perp$ 2.0655) of the related, recently reported Mo(I)/Mo(0) mixed-valent compound $\{(\mu\text{-pz})[\mathrm{Mo(CO)_3(P^iPr_3)_2}]_2\}^+$, pz = pyrazine [18b,c]; the $g_\parallel$ values, on the other hand, are comparable at about 1.97. This result may be due to different geometrical deviations from ideal octahedral symmetry, however, it is probably also a consequence of the more pronounced metal character of the singly occupied MO in $\mathbf{1}^+$ because of only two 'covalent' bonds to CO from each metal instead of three in the mentioned pyrazine-bridged complex. Chelate ligand-bridge $4d^5/4d^6$ mixed-valent systems completely without backdonating co-ligands such as **3** display a still more pronounced *g* anisotropy [23].

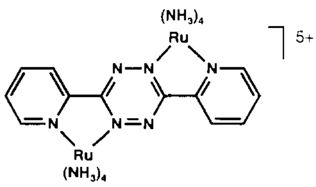

3

Carbonyl vibrational spectroscopy and spectroelectrochemistry have frequently been used to study the effects of one-electron reduction or oxidation [41] or of (de)localization in symmetrical mixed-valent systems [42]. Given the clear evidence from EPR about the electronic structures of anions and cations we obtained the corresponding ν(CO) data in order to evaluate this method for the question of electronic delocalization and oxidation state assignment. The results summarized in Table 2 show the expected [18c,41,42] shifts of ν(CO) to lower energies on reduction and to higher energies on oxidation of **1**; furthermore, the complete disappearance of $Mo^0(CO)_2$ features on oxidation to **1**$^+$ strongly suggests a valence-delocalized species Mo(0.5)/Mo(0.5) on the vibrational time scale [18b,c,42] (Class III behavior [31]).

It is surprising however, that the difference $\Delta\nu$(CO) between **1** and the corresponding anion with its bpym-centered SOMO is about the same as that of the cation with its carbonylmetal-based spin. Evidently, the carbonyl vibrational frequencies are not directly useful in determining the predominant site of electron transfer (metals or ligands), specific metal–carbonyl bonding effects probably being responsible for that situation. The splitting of the two dicarbonylmetal bands (b_{1u}, b_{2u}) is not very variable; it is largest for the cation and smallest for the neutral complex **1**.

The UV–Vis–NIR spectroelectrochemical results are straightforward in the case of the reduction of **1**; the positions, shapes and intensities of the new bands for **1**$^{\bullet-}$ are very similar to those of the bis(tetracarbonylmolybdenum) analogue (Table 5). Electron transfer to the ligand π^* orbital reduces the intensity of the MLCT band (the target orbital is now singly occupied) and shifts this transition to higher energy because of strongly increased ligand donor strength and thus stabilized d orbitals [30].

On oxidation, all three well discernible long-wavelength bands of **1** shift to higher energies, especially the MLCT1 feature. Such a behavior is not unexpected for MLCT bands in dinuclear complexes which undergo an oxidation to the mixed-valent state [18c,43]; it simply reflects the stabilization of d orbitals on oxidation. In view of the similar relative intensities, ligand and solvent sensitivities, we assign the MLCT1 and MLCT2 bands, respectively, as listed in Table 5. In agreement with a previous detailed study on (bpym)$[M(CO)_4]_2$, M = Mo, W [34], we have to identify the MLCT1 band with the $d_{xy} \rightarrow a_u$ transition and the more intense MLCT2 band with the $d_{xz} \rightarrow b_{2u}$ transition although it is clearly the b_{2u} orbital which is the singly occupied MO in the anion **1**$^{\bullet-}$. This orbital reversal between the excited versus the reduced state would explain the negative χ values according to Eq. (2) because the 'redox' orbital b_{2u} of the anionic state would then not be identical with the 'optical' target orbital a_u of the lowest-lying MLCT excited state.

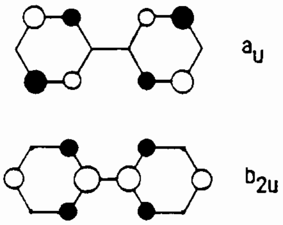

Mixed-valent complexes like **1**$^+$ with similar and potentially interacting metal sites should be distinguished by a special, usually long-wavelength absorption band which may be described as an MMCT or intervalence transition (IT) in the localized formulation, here Mo(I)/Mo(0), or as a transition between two different metal MO combinations in the delocalized form, here Mo(0.5)/Mo(0.5) [18c,21,43,44]. The intensity and energy of such bands has often been indiscriminately correlated with the electrochemically determined comproportionation constant, K_c, regardless of differences in the metal–ligand orbital orientation; however, our recent results on complex **3** showed a rather weak, apparently overlap-disfavored MMCT band at 1453 nm (ϵ 500 M^{-1} cm^{-1}) despite an enormous K_c value of 10^{15} [23]. It was not completely unexpected, therefore, to finally discover the MMCT feature of **1**$^+$ with its smaller K_c of 6×10^8 as a rather weak band at very low energies of 2700 cm^{-1}, corresponding to 3700 nm, in the MIR region (Fig. 7). While the molar extinction could not be determined in this case, the bandwidth at half-height $\Delta\nu_{1/2}$ of about 1300 cm^{-1} is fully compatible with the expected electronic transition [18c,21,43].

Both the energy and the intensity of the MMCT transition of the mixed-valent cation **1**$^+$ are thus unusually small, despite the fact that the electrochemical constant K_c is at least as large as that of the Creutz–Taube ion, $\{(\mu\text{-pz})[Ru(NH_3)_5]_2\}^{5+}$ [21,43–45]. As pointed out previously [23], the relation between K_c and optical data is only valid for compounds with comparable metal–ligand interfaces, i.e. with similar orbital overlap features. As **3** and now **1**$^+$ show, the situation in bis(chelate) ligand-bridged systems is very different from that in the more familiar non-chelate ligand-bridged complexes of the kind of the Creutz–Taube ion [18c,21,43–45]. In both instances, however, a three-site model [5,44] can describe the interaction between two metal centers and a bridging ligand system with low-lying π^* acceptor orbitals; bridging by π electron-donating ligands such as bis(chelating) diacylhydrazido compounds leads to very different spectroscopic effects [5,22,46].

4. Experimental

4.1. Materials and syntheses

2,2′-Bipyrimidine was used as commercially available; 2,5-bppz [47], (2,5-bppz)$[Mo(CO)_4]_2$ [11] and $Mo(CO)_2(PBu_3)_3(CH_3CN)$ [48] were prepared according to literature procedures.

4.1.1. *(μ-bpym)[Mo(CO)$_2$(PBu$_3$)$_2$]$_2$ (1)*

135 mg (0.85 mmol) 2,2′-bipyrimidine and 1400 mg (1.74 mmol) acetonitriledicarbonyltris(tri-n-butylphosphine)molybdenum(0) were suspended in 25 ml hexane. Immediate formation of a blue–purple color indicated the rapid reaction via the mononuclear complex [8]. After 3 h the solution was slowly concentrated in vacuo to about 5 ml and the precipitated complex was filtered from the solution to give the dark, highly soluble material in 60% yield. *Anal.* Found: C, 55.95; H, 9.13; N, 4.06. Calc. for $C_{60}H_{114}Mo_2N_4O_4P_4$ (1271.4): C, 56.68; H, 9.04; N, 4.41%.

4.1.2. *(μ-bppz)[Mo(CO)$_2$(PBu$_3$)$_2$]$_2$ (2)*

200 mg (0.85 mmol) 2,5-di(2-pyridyl)pyrazine and 1400 mg (1.74 mmol) $Mo(CO)_2(PBu_3)_3(CH_3CN)$ were reacted in 100 ml hexane. After 180 min the solvent was removed to yield a dark and very sensitive, non-crystalline material in about 50% yield. ^{1}H NMR spectroscopy (Table 1) showed the formation of **2** but suggested also that small amounts of free PBu_3 were responsible for the reluctance to crystallization. Attempts to remove PBu_3 by extraction with hexane remained unsuccessful; an elemental analysis of the extremely air-sensitive viscous product was not possible.

4.2. *Instrumentation*

EPR spectra were recorded in the X band on a Varian E9 spectrometer and on a Bruker System ESP 300, equipped with a Bruker ER035M gaussmeter and an HP 5350B microwave counter. NMR spectra were taken on a Bruker WH 270 spectrometer. Cyclic voltammetry was carried out in dry DMF, dichloromethane or 1,2-dichloroethane (DCE)/0.1 M Bu_4NClO_4, using a three-electrode configuration (glassy carbon working electrode, SCE reference, Pt counter electrode) and a PAR 273/175 potentiostat/function generator. For complex **1** the ferrocene/ferrocenium couple $FeCp_2^{0/+}$ was used as internal standard (Fig. 3).

IR spectra were measured on Perkin-Elmer 684 and Philips PU9800 FTIR systems, UV–Vis–NIR spectra were recorded on a Bruins Instruments Omega 10 spectrophotometer. EPR [49], UV–Vis–NIR and IR spectroelectrochemistry [29] was performed using previously described cells and CH_2Cl_2/0.1 M Bu_4NPF_6 as electrolyte.

Acknowledgements

This work has been supported by grants from the Deutsche Forschungsgemeinschaft (DFG), Volkswagenstiftung, Fonds der Chemischen Industrie and an Exchange Program between DFG and the Academy of Sciences of the Czech Republic.

References

[1] M. Matsuoka (ed.), *Infrared Absorbing Dyes*, Plenum, New York, 1990.

[2] J. Fabian and R. Zahradnik, *Angew. Chem., 101* (1989) 693; *Angew. Chem., Int. Ed. Engl., 28* (1989) 677.

[3] (a) G.N. Schrauzer, *Acc. Chem. Res., 2* (1969) 72; (b) W. Kaim, S. Ernst and S. Kohlmann, *Polyhedron, 5* (1986) 445; (c) K. Yoshida, N. Oga, M. Kadota, Y. Ogasahara and Y. Kubo, *J. Chem. Soc., Chem. Commun.*, (1992) 1114; (d) M. Emmelius, G. Pawlowski and H. Vollmann, *Angew. Chem., 101* (1989) 1475; *Angew. Chem., Int. Ed. Engl., 28* (1989) 1445.

[4] O. Horvath and K.L. Stevenson, *Charge Transfer Photochemistry of Coordination Compounds*, VCH, Weinheim, Germany, 1993.

[5] W. Kaim and V. Kasack, *Inorg. Chem., 29* (1990) 4696.

[6] S.D. Ernst and W. Kaim, *Inorg. Chem., 28* (1989) 1520.

[7] H. tom Dieck, K.D. Franz and F. Hohmann, *Chem. Ber., 108* (1975) 163.

[8] S. Ernst, S. Kohlmann and W. Kaim, *J. Organomet. Chem., 354* (1988) 177.

[9] (a) L.H. Staal, D.J. Stufkens and A. Oskam, *Inorg. Chim. Acta, 26* (1978) 255; (b) R. Balk, D.J. Stufkens and A. Oskam, *Inorg. Chim. Acta, 28* (1978) 133.

[10] (a) S.W. Lee and W.C. Trogler, *Organometallics, 9* (1990) 1470; (b) W.C. Trogler, *Acc. Chem. Res., 23* (1990) 426.

[11] W. Kaim and S. Kohlmann, *Inorg. Chem., 26* (1987) 68.

[12] S. Ernst, V. Kasack and W. Kaim, *Inorg. Chem., 27* (1988) 1146.

[13] E.S. Dodsworth and A.B.P. Lever, *Coord. Chem. Rev., 97* (1990) 271.

[14] (a) W. Matheis and W. Kaim, *Inorg. Chim. Acta, 181* (1991) 15; (b) C. Vogler, H.-D. Hausen, W. Kaim, S. Kohlmann, H.E.A. Kramer and J. Rieker, *Angew. Chem., 101* (1989) 1734; *Angew. Chem., Int. Ed. Engl., 28* (1989) 1659; (c) C. Vogler, W. Kaim and H.-D. Hausen, *Z. Naturforsch., Teil B, 48* (1993) 1470; (d) J.-A. Real, H. Bolvin, A. Bousseksou, A. Dworkin, O. Kahn, F. Varret and J. Zarembowitch, *J. Am. Chem. Soc., 114* (1992) 4650; (e) G. De Munno, M. Julve, F. Nicolo, F. Lloret, J. Faus, R. Ruiz and E. Sinn, *Angew. Chem., 105* (1993) 588; *Angew. Chem., Int. Ed. Engl., 32* (1993) 613.

[15] (a) S. Campagna, G. Denti, G. De Rosa, L. Sabatino, M. Ciano and V. Balzani, *Inorg. Chem., 28* (1989) 2565; (b) G. Denti, S. Serroni, S. Campagna, V. Ricevuto and V. Balzani, *Inorg. Chim. Acta, 182* (1991) 127.

[16] (a) A. Das, C. Jeffery, J.P. Maher, J.A. McCleverty, E. Schatz, M.D. Ward and G. Wollermann, *Inorg. Chem., 32* (1993) 2145; (b) A.J. Amoroso, J.P. Maher, J.A. McCleverty and M.D. Ward, *J. Chem. Soc., Chem. Commun.*, (1994) 1273.

[17] (a) C.J. Casewit and M. Rakowski-DuBois, *Rev. Inorg. Chem., 9* (1988) 199; (b) C.G. Young, *Coord. Chem. Rev., 96* (1989) 89.

[18] (a) W. Bruns, W. Kaim, M. Ladwig, B. Olbrich-Deussner, T. Roth and B. Schwederski in A.J.L. Pombeiro and J. McCleverty (eds.), *Molecular Electrochemistry of Inorganic, Bioinorganic and Organometallic Compounds*, Kluwer, Dordrecht, Netherlands, 1993, p. 255; (b) W. Bruns, W. Kaim, E. Waldhör and M. Krejčik, *J. Chem. Soc., Chem. Commun.*, (1993) 1868; (c) W. Bruns, W. Kaim, E. Waldhör and M. Krejčik, *Inorg. Chem.*, in press.

[19] A. Bino, F.A. Cotton, D.O. Marler, S. Farquharson, B. Hutchinson, B. Spencer and J. Kincaid, *Inorg. Chim. Acta, 133* (1987) 295.

[20] F.A. Cotton and R.A. Walton, *Multiple Bonds between Metal Atoms*, Clarendon, Oxford, 1993, pp. 210–214.

[21] C. Creutz, *Prog. Inorg. Chem., 30* (1983) 1.

[22] W. Kaim, V. Kasack, H. Binder, E. Roth and J. Jordanov, *Angew. Chem., 100* (1988) 1229; *Angew. Chem., Int. Ed. Engl., 27* (1988) 1174.

[23] J. Poppe, M. Moscherosch and W. Kaim, *Inorg. Chem., 32* (1993) 2640.

[24] (a) F.A. Cotton, M. Matusz and B. Zhong, *Inorg. Chem., 27* (1988) 4368; (b) F.A. Cotton and R.A. Walton, *Multiple Bonds between Metal Atoms,* Clarendon, Oxford, 1993, pp. 399–416.

[25] W. Kaim, *Coord. Chem. Rev., 76* (1987) 187.

[26] W. Kaim, *Inorg. Chem., 23* (1984) 3365.

[27] A.D. McLachlan, *Mol. Phys., 3* (1960) 233.

[28] A. Stebler, J.H. Ammeter, U. Fürholz and A. Ludi, *Inorg. Chem., 23* (1984) 2764.

[29] M. Krejčik, M. Danek and F. Hartl, *J. Electroanal. Chem., 317* (1991) 179.

[30] P.S. Braterman, J.-I. Song, S. Kohlmann, C. Vogler and W. Kaim, *J. Organomet. Chem., 411* (1991) 207.

[31] M.B. Robin and P. Day, *Adv. Inorg. Chem. Radiochem., 10* (1967) 247.

[32] S.P. Best, R.J.H. Clark, C.S. McQueen and S. Joss, *J. Am. Chem. Soc., 111* (1989) 548.

[33] N. Juranic, *Coord. Chem. Rev., 96* (1989) 253, and refs. therein.

[34] W. Kaim, S. Kohlmann, A.J. Lees, T.L. Snoeck, D.J. Stufkens and M.M. Zulu, *Inorg. Chim. Acta, 210* (1993) 159.

[35] (a) K.J. Moore and J.D. Petersen, *Polyhedron, 2* (1983) 279; (b) C. Overton and J.A. Connor, *Polyhedron, 1* (1982) 53.

[36] D.P. Rillema and K.B. Mack, *Inorg. Chem., 21* (1982) 3849.

[37] (a) E. Dodsworth and A.B.P. Lever, *Chem. Phys. Lett., 124* (1986) 152; (b) E.M. Kober, K.A. Goldsby, D.N.S. Narayana and T.J. Meyer, *J. Am. Chem. Soc., 105* (1983) 4303.

[38] W. Matheis and W. Kaim, *J. Chem. Soc., Faraday Trans., 86* (1990) 3337.

[39] (a) K. Prassides (ed.), *Mixed Valency Systems – Applications in Chemistry, Physics and Biology,* Kluwer, Dordrecht, Netherlands, 1991; (b) W. Kaim, W. Bruns, J. Poppe and V. Kasack, *J. Mol. Struct., 292* (1993) 221.

[40] J.C. Giordan, J.H. Moore, J.A. Tossell and W. Kaim, *J. Am. Chem. Soc., 107* (1985) 5600.

[41] (a) R.E. Dessy, J.C. Charkoudian, T.B. Abeles and A.L. Rheingold, *J. Am. Chem. Soc., 92* (1970) 3947; (b) Y. Zhang, D.K. Gosser, P.H. Rieger and D.A. Sweigart, *J. Am. Chem. Soc., 113* (1991) 4062.

[42] (a) C.G. Atwood and W.E. Geiger, *J. Am. Chem. Soc., 115* (1993) 5310; (b) W.E. Geiger, N. Van Order, Jr., D.T. Pierce, T.E. Bitterwolf, A.L. Rheingold and N.D. Chasteen, *Organometallics, 10* (1991) 2403.

[43] P.A. Lay, R.H. Magnuson and H. Taube, *Inorg. Chem., 27* (1988) 2364.

[44] (a) L.T. Zhang, J. Ko and M.J. Ondrechen, *J. Am. Chem. Soc., 109* (1987) 1666 and 1674; (b) V. Petrov, J.T. Hupp, C. Mottley and L.C. Mann, *J. Am. Chem. Soc., 116* (1994) 2171.

[45] D.E. Richardson and H. Taube, *J. Am. Chem. Soc., 105* (1983) 40.

[46] V. Kasack, W. Kaim, H. Binder, J. Jordanov and E. Roth, *Inorg. Chem.,* submitted for publication.

[47] F.H. Case and E. Koft, *J. Am. Chem. Soc., 81* (1959) 905.

[48] H. tom Dieck and H. Friedel, *J. Organomet. Chem., 14* (1968) 375.

[49] W. Kaim, S. Ernst and V. Kasack, *J. Am. Chem. Soc., 112* (1990) 173.